High-resolution postmortem 7 tesla MRI yields localized atrophy measures that are more sensitive to tau pathology and neuronal loss in Alzheimer's disease than corresponding measures on antemortem 3 tesla MRI

Pulkit Khandelwal, Michael Tran Duong, Lisa Levorse, Sydney A. Lim, Amanda E. Denning, Nathaniel Gauthier, Ved Shenoy, Winifred Trotman, Ranjit Ittyerah, Alejandra Bahena, Theresa Schuck, Marianna Gabrielyan, Karthik Prabhakaran, Daniel T. Ohm, Gabor Mizsei, John Robinson, John A. Detre, Edward B. Lee, David J. Irwin, Corey McMillan, M. Dylan Tisdall, Sandhitsu R. Das, David A. Wolk, and Paul A. Yushkevich
University of Pennsylvania, USA

Background: Postmortem MRI has opened-up avenues to study brain structure at sub-millimeter ultra high-resolution revealing details not possible to observe with in vivo MRI. Here, we present a novel package (purple-mri) which performs segmentation, parcellation and registration of postmortem MRI. Additionally, we provide a framework to perform one-of-its-kind vertex-wise group-level studies linking morphometry/histopathology in common coordinate system for postmortem MRI.

Method: We developed a combined voxel- and surface-based pipeline combining deep learning with classical techniques for topology correction, cortical modeling, inflation, registration for accurate parcellation of postmortem cerebral hemispheres (Fig.1 Khandelwal et al. 2024). Moreover, using the GM/WM segmentations derived from postmortem hemisphere and FreeSurfer-processed antemortem MRI, we perform deformable image registration between the two modalities for each brain specimen. Vertex-wise thickness analysis was performed to assess tau and neuronal loss distribution in corresponding specimens of postmortem (7T at 0.3mm^3; N=75) and antemortem (3T at 0.8mm^3; N=49) MRI (Table 1) with AD continuum diagnosis. The semi-quantitative average tau and neuronal loss ratings were derived from histopathological examination across the brain. All analyses include age, sex, and postmortem (or antemortem) interval as covariates.

Result: Our method parcellates postmortem brain hemisphere using a variety of brain atlases even in areas with low contrast (anterior/posterior regions), profound imaging artifacts and severe atrophied brains (Fig. 1). Our registration pipeline provides one-to-one correspondence between the two modalities. For thickness/pathology associations, small sparse significant clusters in superior temporal and precuneus in antemortem MRI (N=49) were observed. However, postmortem MRI showed much stronger associations across large clusters in the temporal, entorhinal cortex, and cingulate for both the matched cases (N=49) and the full cohort (N=75), regions implicated in ADRD.

Conclusion: Purple-mri paves the way for large-scale postmortem image analysis. Stronger associations between thickness and average tau burden/neuronal loss than antemortem MRI shows that our pipeline (purple-mri) could inform the development of more precise and sensitive invivo biomarkers by mapping information from postmortem to antemortem MRI in a common reference coordinate framework just as is the norm for antemortem studies.

Table 1. Demographics of the Alzheimer's disease and related dementias (ADRD) specimens. Abbreviations: PART: Primary age-related tauopathy; LATE: Limbic-predominant age-related TDP-43 encephalopathy.

Brain donor cohort				
N	75 (Female: 37 and Male: 38)			
Age (years)	76.56 ± 10.61 (range 53-101)			
Race	White: 68 Black: 6 More than one race: 1			
Hemisphere imaged	Right: 35 Left: 40			
Postmortem interval (hours)	19.06 ± 13.93 (range: 3-84)			
Fixation time (days)	244.16 ± 282.98 (range: 29-1178)			
Antemortem interval (years)	6.08 ± 4.26 (range: 0.27-15.39)			
Neuropathological diagnosis				
	Primary		**Secondary/ tertiary**	
Alzheimer's disease	47		19	
Lewy body disease	20		21	
Cerebrovascular disease	3		2	
Globular glial tauopathy	2		-	
PART	1		5	
Hippocampal Sclerosis	-		1	
LATE	2		14	
Global neuropathological staging				
Ratings	**0**	**1**	**2**	**3**
Amyloid-β Thal staging (A score)	7	6	15	47
Braak three stage scheme (B score)	0	16	16	43
CERAD (C score)	16	4	11	44

Figure 1. We have developed and released a package (purple-mri: Penn Utilities for Registration and ParcelLation of Ex vivo MRI) which performs image segmentation, parcellation and registration for high resolution postmortem MRI to help link structural changes with histopathological measures enabling the study of pathology/structure associations in the human brain. Shown below are segmentations of the postmortem brain hemispheres imaged at 0.3mm^3 using 7 tesla MRI for two subjects (A and B) using the FreeSurfer DKT atlas. The corresponding antemortem MRI (imaged at 0.8mm^3 using 3 tesla MRI) was registered to the postmortem hemisphere. The antemortem MRI was segmented using the DKT atlas via FreeSurfer. Our pipeline also parcellates the postmortem brain hemisphere using a variety of atlases as shown in panel C. Our method parcellates the brain consistently with the in vivo approach even in regions where the ex vivo MR signal contrast is low in the anterior and the posterior due to MRI coil-related artifacts.

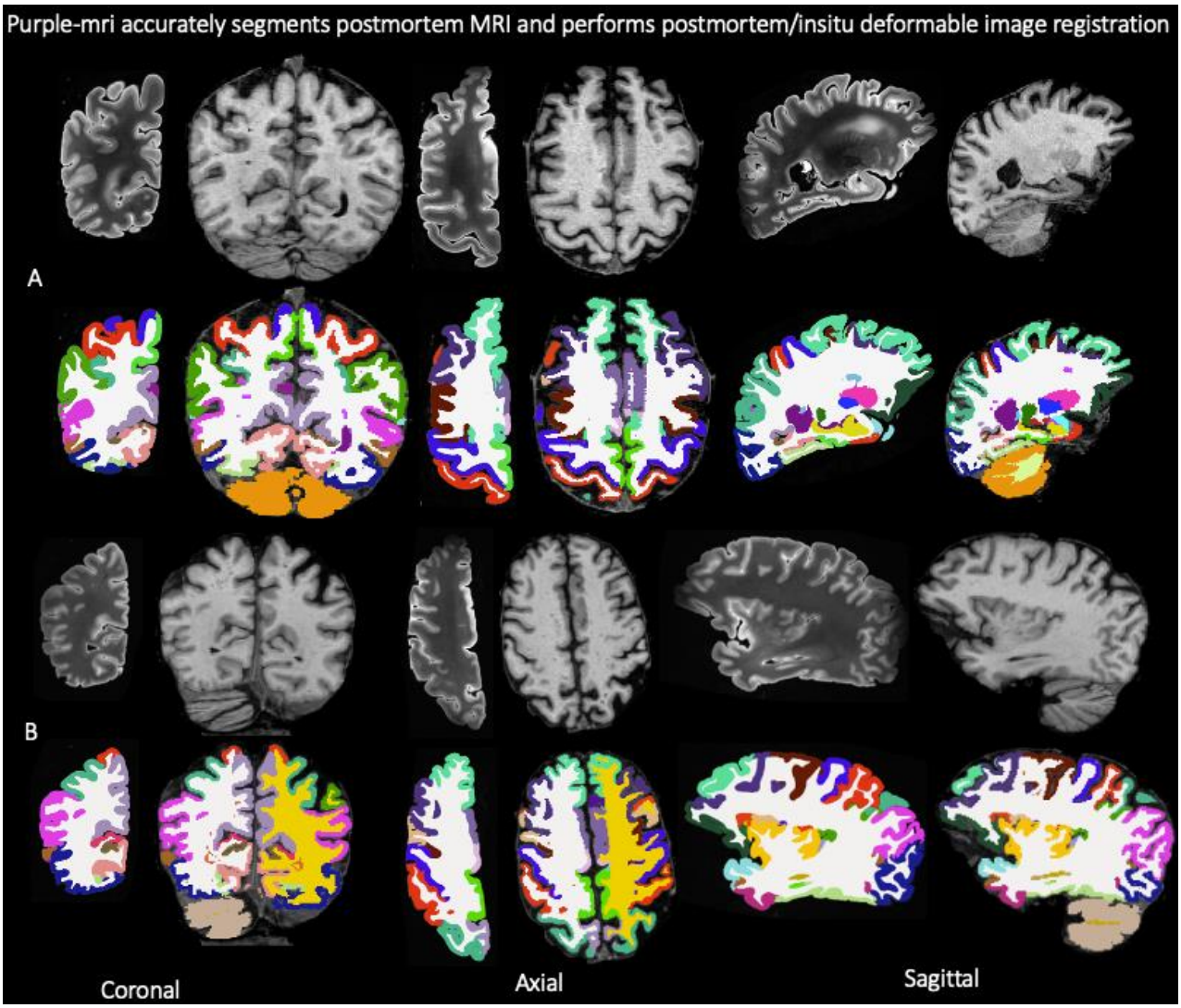

Purple-mri provides postmortem hemisphere MRI parcellations for a variety of atlases

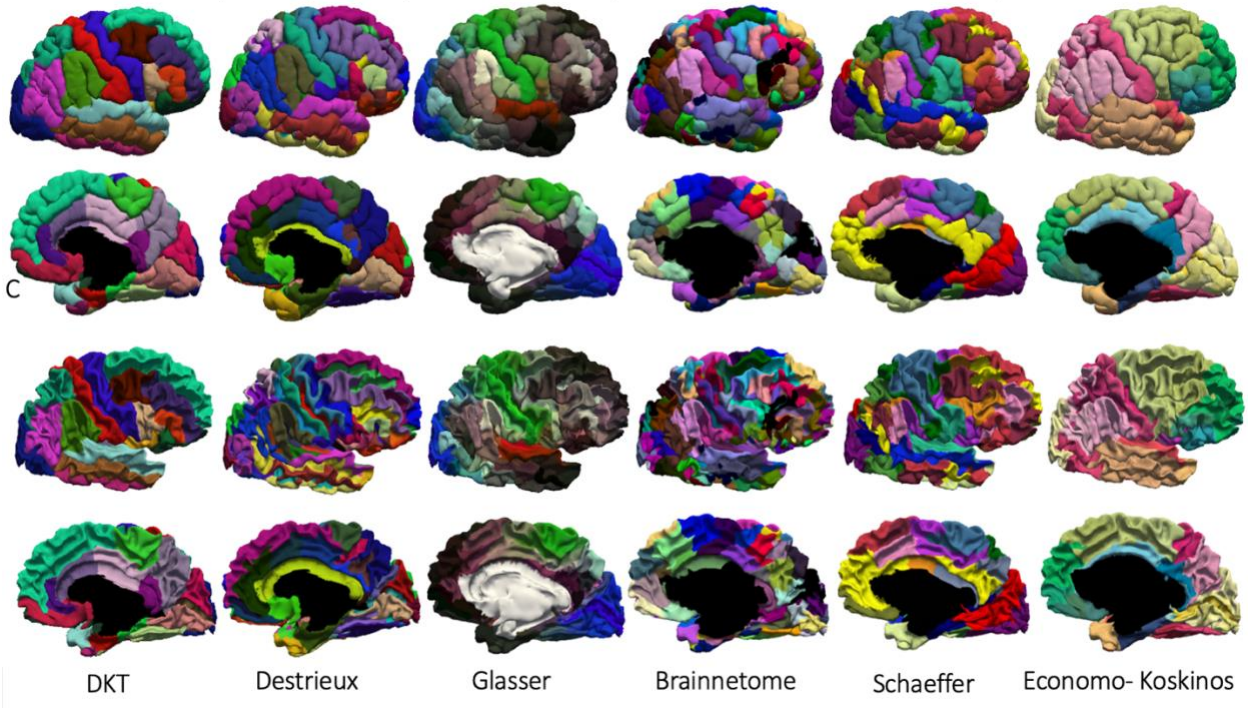

Figure 2. Template-space vertex-wise morphometry-pathology correlations. The thickness maps for each individual subject were warped to the fsaverage template-space (provided in FreeSurfer) for vertex-wise correlation analysis between cortical thickness (mm) and the whole-hemisphere average tau burden and neuronal loss ratings. The average tau burden and neuronal loss ratings were obtained by averaging the pathologists' semiquantitative pathology ratings (scale of 0–3, "0: None," "0.5: Rare," "1: Mild," "2: Moderate," or "3: Severe") from 8 sampling locations in the contralateral hemisphere. The sampling locations were: amygdala, angular gyrus, cingulate gyrus, middle frontal gyrus, occipital cortex, superior/middle temporal, and medial temporal lobe (defined as the average of ratings in CA1/subiculum, dentate gyrus, and entorhinal cortex). Vertex-wise correlation between thickness and the tau burden and neuronal loss ratings was performed by fitting a general linear model (GLM) at each vertex, using threshold-free cluster enhancement (TCFE), with thickness as the dependent variable; tau burden or neuronal loss as the independent variable of interest; age, sex and PMI (AMI for antemortem MRI) as nuisance covariates and corrected for multiple comparisons using family-wise error rate (FWER) correction. Shown are the strongest associations (corrected $p<0.1$) for the antemortem (N=49), postmortem (N=49 cases matched to the antemortem cohort), and for the full postmortem (N=75) cohort. The affine transformation which was obtained via postmortem/antemortem MRI registration was applied on the postmortem hemispheres in the (N=49) cohort. This transformation accounts for the deformation introduced in postmortem brain specimens due to fixation artifacts and additional atrophy between the antemortem scan and death. Abbreviations: AMI: antemortem interval; PMI: postmortem interval.

Generalized linear modeling: vertex-wise thickness (mm) vs neuropathology ratings